Supplementary information for

On pathways of heterogeneous catalytic decarbonylation of lactic acid to acetaldehyde

Lin Huang,* Chuan Wang, De Sheng Theng and Lili Zhang
Institute of Sustainability for Chemicals, Energy and Environment, Agency for Science, Technology and Research, 1 Pesek Road, Jurong Island, Singapore 627833, Singapore. E-mail: huanglin@awfa.com.sg

Acid properties of catalyst systems

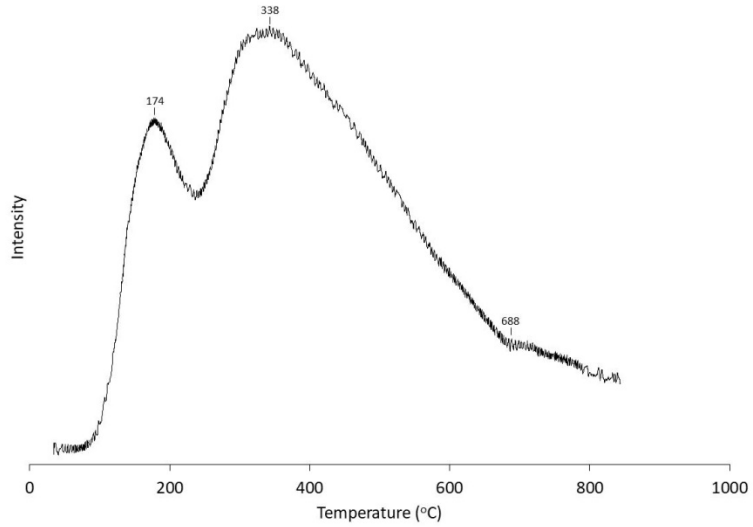

Fig. S1 NH_3-TPD profile of the commercial Na-SiO_2-Al_2O_3(15).

Catalytic properties in the vapour-phase decarbonylation of LA

Table S1 Catalytic properties in the vapour-phase decarbonylation of LA over the Na-SiO_2-Al_2O_3(35) at 330-370 °C. [a]

T (°C)	Conversion (%)	AD yield (%)	Selectivity (%)		Sel. AD /Sel. AA
			AD	AA	
330	70	13	19	22	0.86
350	85	25	27	30	0.90
370	100	34	34	32	1.1

[a] 0.50 g of precatalyst, 20 % LA aqueous solution, $WHSV_{LA}$ = 0.50 h^{-1}, carrier gas flow rate = 30 ml min^{-1}, data taken after 5 h of reaction.

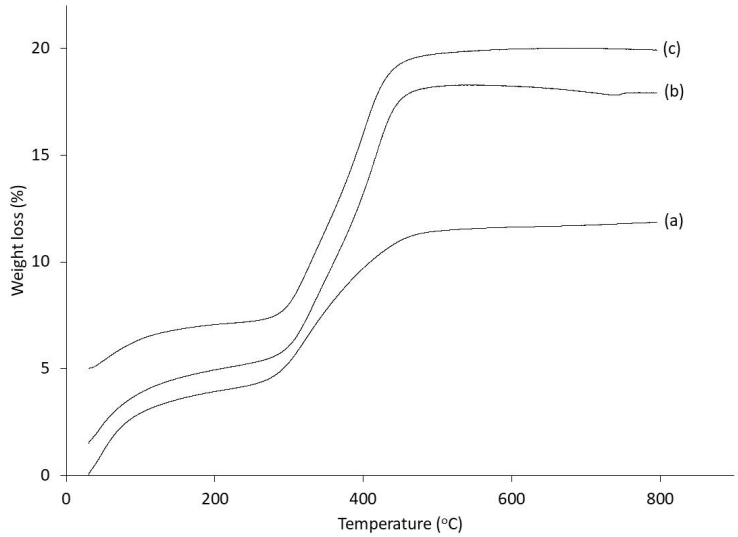

Fig. S2 Thermogravimetric profiles in air of the spent Na-SiO_2-Al_2O_3(35) catalyst samples after the LA decarbonylation at 350 °C for (a) 5 h, (b) 28 h and (c) 50 h.

Reaction intermediates of the LA decarbonylation on catalyst systems

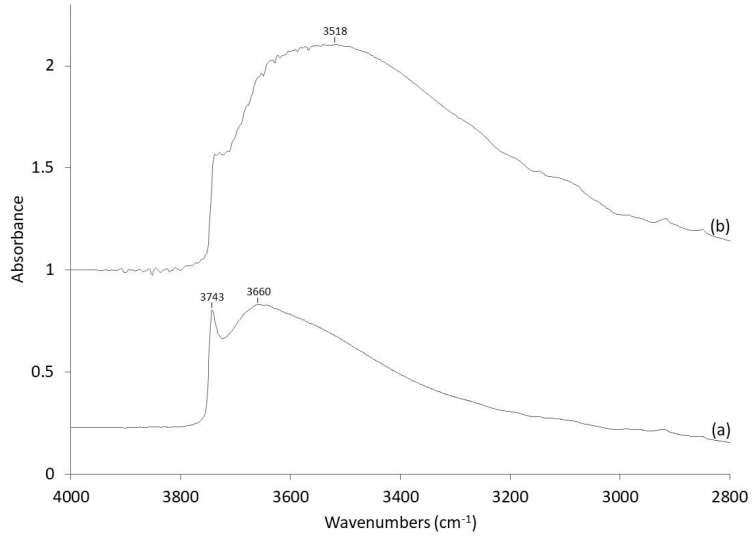

Fig. S3 Surface IR spectra before (a) and after (b) deionized water reaction on the H-SiO_2-Al_2O_3(35) at 22 °C for 30 min under vacuum.

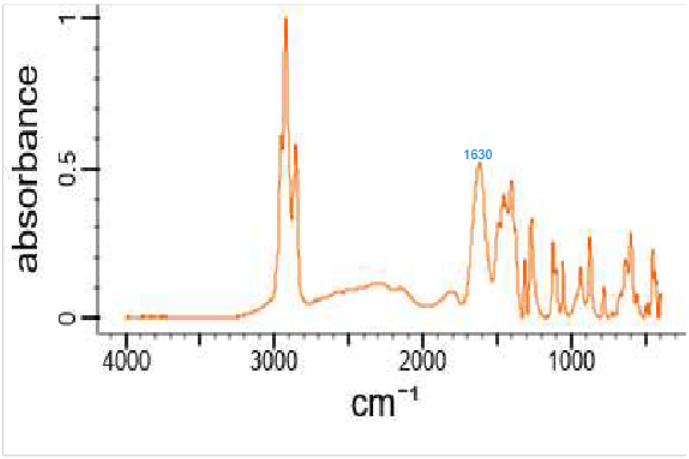

Properties

SpectraBase Spectrum ID	IOMD1KKJ8eH
Name	Aluminum L-lactate
Source of Sample	Aldrich
Catalog Number	430633
Classification	Non-aromatic acid salts
Copyright	Copyright © 2018-2024 Sigma-Aldrich Co. LLC. - Database Compilation Copyright © 2018-2024 John Wiley & Sons, Inc. All Rights Reserved.
Formula	C9H15AlO9
InChI	InChI=1S/3C3H6O3.Al/c3*1-2(4)3(5)6;/h3*2,4H,1H3,(H,5,6);/q;;;+3/p-3/t3*2-;/m000./s1
InChIKey	VXYADVIJALMOEQ-LGISMKCISA-K
Purity	95%
Solvent	Nujol
Source of Spectrum	Sigma-Aldrich Co. LLC.
Synonyms	L-Lactic acid aluminum salt

Fig. S4 IR spectrum of aluminium L-lactate.[34]

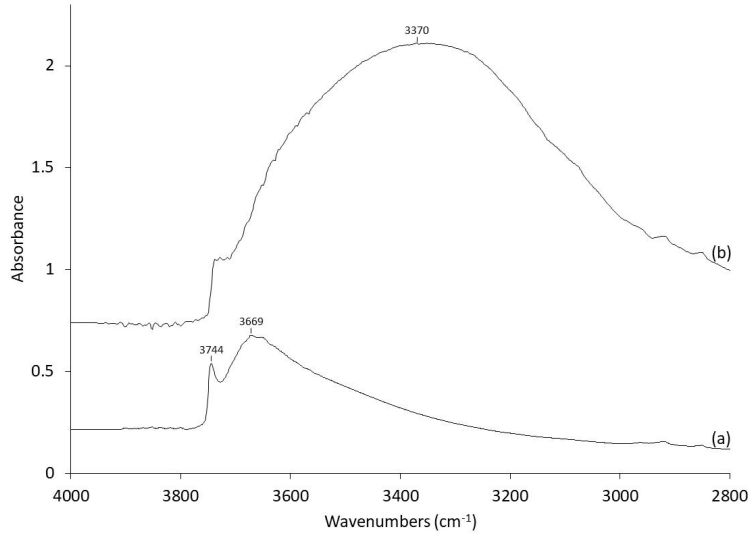

Fig. S5 Surface IR spectra before (a) and after (b) deionized water reaction on the Grade 15 SiO_2 at 22 °C for 30 min under vacuum.

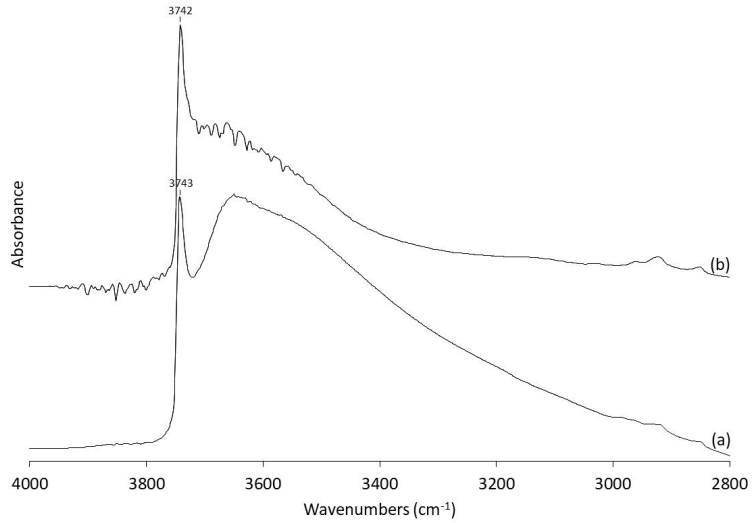

Fig. S6 Surface IR spectra of (a) the H-SiO_2-Al_2O_3(35) and (b) Na-SiO_2-Al_2O_3(35).

In the case with the Na-SiO_2-Al_2O_3(23), it seems that the lower Si/Al molar ratio of 23, *i.e.*, a moderate surface acidity, results in better separation of surface carbonyl spectra. In fact, the moderate surface acidity appeared to speed up hydrolysis of *in situ* generated lactates and polymerization of LA while slowing down dehydration of LA. As shown in Fig. S7(a), a principal band of sodium lactate became invisible quickly at 22 °C, which was accompanied by the appearance of a principal band of LA at 1726(s) cm^{-1}. Apparently, the sodium lactate hydrolyzes preferentially to the surface silican and

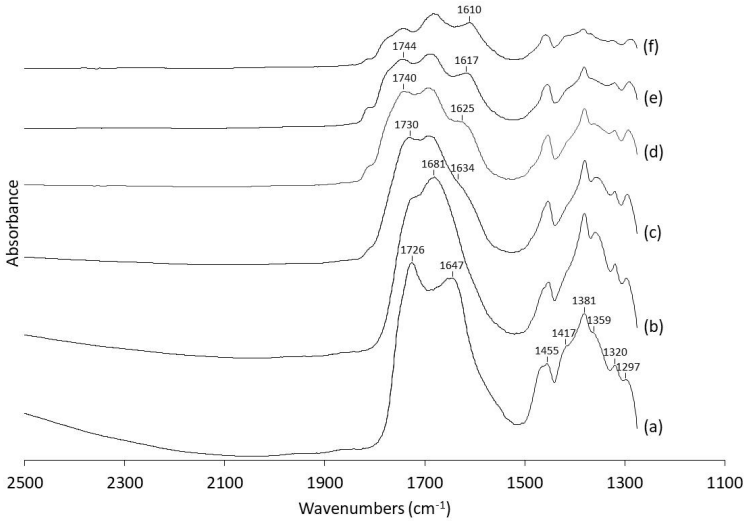

Fig. S7 Subtract surface IR spectra after LA reaction on the Na-SiO_2-Al_2O_3(23) at (a) 22 °C for 0.5 h under vacuum, (b) 100 °C for 0.5 h under N_2, (c) 200 °C for 0.5 h under N_2, (d) 300 °C for 0.5 h under N_2, (e) 350 °C for 0.5 h under N_2 and (f) 350 °C for 4 h under N_2.

aluminium lactates under the moderately acidic condition, as expected. With increasing temperature up to 200 °C, the hydrolysis of the lactates kept proceeding with the concomitant occurrence of the decarbonylation and dehydration of the LA. Probably due to the higher decarbonylation/dehydration rate ratio, less amounts of AA were produced so that the separate bands of the LA at 1726 - 1730 cm^{-1} and the strongly physisorbed LA at 1681 cm^{-1} were observed, as in Figs. S7(b) and S7(c). Above 100 °C, the 1730 and 1681 cm^{-1} bands reduced as the decarbonylation and dehydration were reinforced. As the 1681 cm^{-1} band reduced, the principal band of the lactates became visible at 1634 cm^{-1} at 200 °C. Above 200 °C, the 1730 cm^{-1} band shifted to 1744 cm^{-1} while reducing. The latter band can be considered to be overlapped of those of the PLA and LA, implying that the LA polymerization takes place to a moderate extent. Meanwhile the continuous reduction in the 1681 cm^{-1} band rendered the 1634 cm^{-1} band progressively shift to 1610 cm^{-1}, as in Figs. S7(d) – S7(f). From the spectral evolution in the process, the bands of the PLA, LA and strongly physisorbed LA continuously reduce whereas that of the lactates remains substantially unchanged in intensity even after 4 h of heating at 350 °C. This is spectroscopic evidence of the stabilization of the lactates on the moderate solid acid towards the LA decarbonylation. The fair chemical stability of the lactates is confirmed by the spectrum of a spent Na-SiO_2-Al_2O_3(23) catalyst sample after 28 h of LA decarbonylation at 350 °C. Principal bands of both surface silicon and aluminium lactates, and sodium lactate were observed at 1631(s) and 1593(sh) cm^{-1}, respectively, as in Fig. 7(d). The 1593(sh) cm^{-1} band is less intense than that of the spent Na-SiO_2-Al_2O_3(35), likely due to the quicker

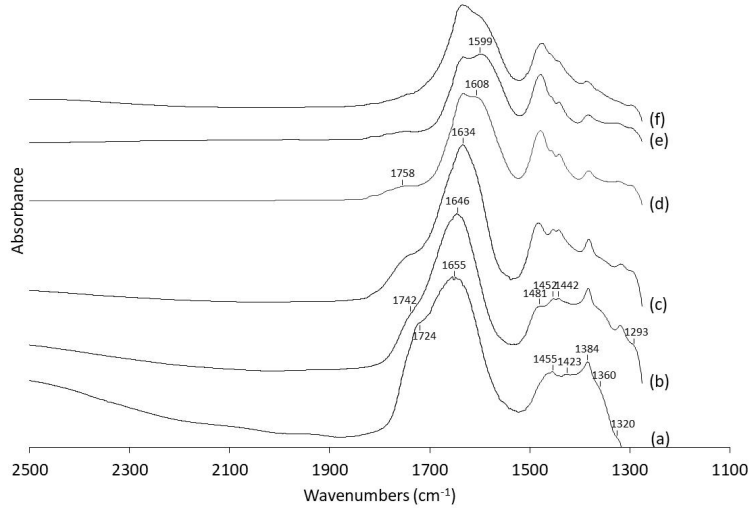

Fig. S8 Subtract surface IR spectra after LA reaction on the Na-SiO_2-Al_2O_3(5) at (a) 22 °C for 0.5 h under vacuum, (b) 100 °C for 0.5 h under N_2, (c) 200 °C for 0.5 h under N_2, (d) 300 °C for 0.5 h under N_2, (e) 350 °C for 0.5 h under N_2 and (f) 350 °C for 2 h under N_2.

hydrolysis of the sodium lactate proceeding over the more acidic Na-SiO_2-Al_2O_3(23). Nonetheless, these results are in agreement with the higher selectivity to PLA + coke and the fair catalytic stability for the production of AD over the moderately acidic Na-SiO_2-Al_2O_3(23).

In the case with the Na-SiO_2-Al_2O_3(5), it appears that the high surface acidity leads to quick LA polymerization and coke formation while producing better separation of surface carbonyl spectra, as in Fig. S8. As a matter of fact, surface reactions seemed to be in a transient equilibrium at 22 °C. Heating up to 200 °C apparently promoted desorption of strongly physisorbed LA and the polymerization of LA, a principal band of LA at 1724(sh) cm^{-1} shifting towards 1758(sh) cm^{-1} and a band at 1655 cm^{-1} shifting up to 1634 cm^{-1} with the concurrent growth of a band at 1481 cm^{-1}. The copresence of the 1634 and 1481 cm^{-1} bands may presumably be associated with aluminium lactate.[34] The 1634 and 1481 cm^{-1} bands are presumably attributed to surface silicon and aluminium lactates. Above 200 °C, the band of the PLA tremendously reduced while those of the surface silicon and aluminium lactates slightly reduced. As the 1634 cm^{-1} band reduced, a band at 1599 cm^{-1} appeared likely as the principal feature of sodium lactate and quickly reduced at 350 °C, as in Figs. S8(e) and S8(f). The spectral observations at this point account for that under the strongly acidic condition, sodium lactate hydrolysis proceeds expectedly faster than surface silicon and aluminium lactate hydrolyses, while the coke formation from PLA proceeds quickly. Since the principal band of poly(sodium acrylate) around 1575 cm^{-1} [81,82] is not visible after 2 h of heating at 350 °C, we deem that in spite of the high acidity of the Na-SiO_2-Al_2O_3(5), sodium lactate dehydration

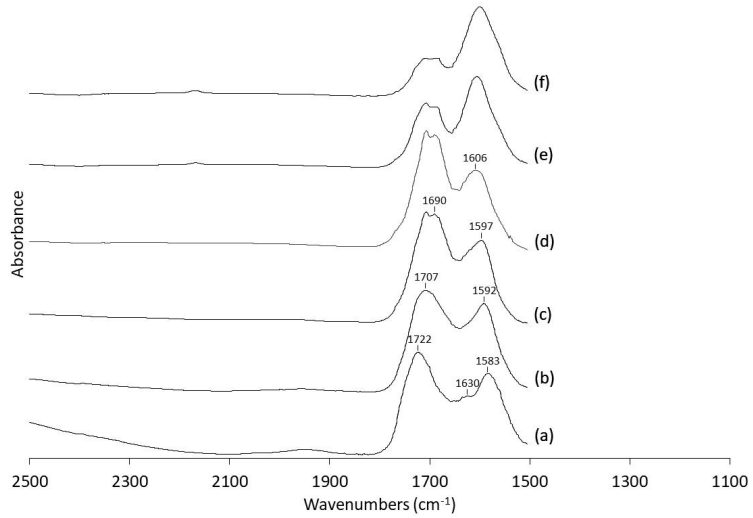

Fig. S9 Subtract surface IR spectra after LA reaction on the $Na(NO_3)_3$/Na-SiO_2-Al_2O_3(35) at (a) 22 °C for 52 min under vacuum, (b) 100 °C for 30 min under N_2, (c) 200 °C for 30 min under N_2, (d) 300 °C for 30 min under N_2, (e) 350 °C for 30 min under N_2 and (f) 350 °C for 240 min under N_2.

takes place to a negligible extent whereas the sodium lactate hydrolysis is responsible for the fall in the content of the sodium lactate. The chemical instability of the lactates is confirmed by the spectra of a spent Na-SiO_2-Al_2O_3(5) catalyst sample after LA decarbonylation at 350 °C. After 5 h of reaction, the spectrum gave a principal band of surface silicon and aluminium lactates at 1631(s) cm^{-1} without that of sodium lactate (Fig. 7(e)), indicating that the strongly acidic condition causes disappearance of the sodium lactate via the quicker hydrolysis. After 28 h of reaction, the 1631 cm^{-1} band considerably decreased in intensity with the concurrent appearance of a 1568 cm^{-1} band likely due to poly(sodium acrylate). This indicates that under the strongly acidic condition, the long-term catalytic reaction eventually leads to loss of the surface silicon and aluminium lactates via the hydrolysis while accumulation of sodium acrylate via the hydrolysis of the sodium lactate followed by AA neutralization with Na^+ triggers polymerization of the sodium acrylate.[21] The chemical instability of the lactates and the quick appearance and disappearance of the PLA are consistent with the high selectivity to PLA + coke and the fast catalyst deactivation, respectively over the strongly acidic Na-SiO_2-Al_2O_3(5).

Based on the cases with the Na-SiO_2-Al_2O_2, let us furthermore go through the case with the $NaNO_3$/Na-SiO_2-Al_2O_3(35). The high sodium loading via the incorporation of $NaNO_3$ evidently leads to the formation of a dominant fraction of sodium lactate over surface silicon and aluminium lactates. Fig. S9 gives subtract surface IR spectra in the 2500-1500 cm^{-1} region during a reaction of LA on the $NaNO_3$/Na-SiO_2-Al_2O_3(35) at 22-350 °C. In light of the reported thermal stability of $NaNO_3$ on SiO_2 and

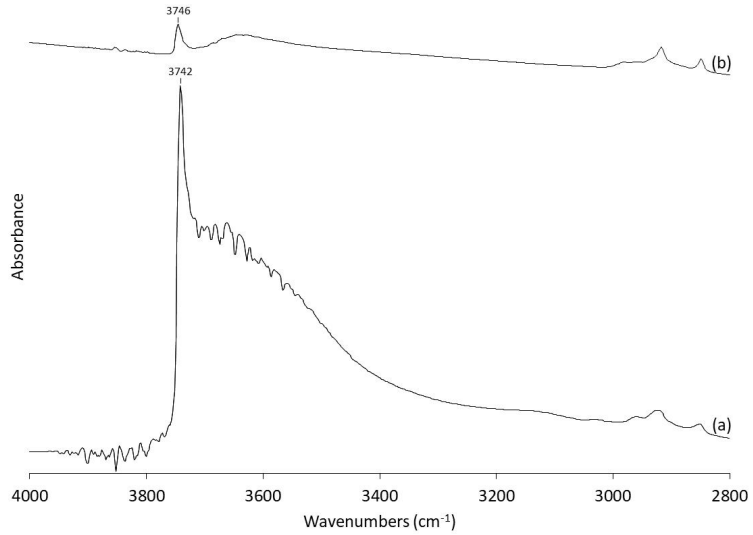

Fig. S10 Surface IR spectra of (a) the Na-SiO_2-Al_2O_3(35) and (b) $Na(NO_3)_3$/Na-SiO_2-Al_2O_3(35).

hydroxyapatite,[83,84] the $NaNO_3$ is deemed to remain intact on the less acidic Na-SiO_2-Al_2O_3(35) regardless of the calcination of the $NaNO_3$/Na-SiO_2-Al_2O_3(35) in air at 540 °C. At 22 °C, a principal band of LA at 1722(s) cm^{-1} was observed together with principal ones of surface silicon and aluminium lactates at 1630(m) cm^{-1} [34] and sodium lactate at 1583(s) cm^{-1}.[76,77] Apparently, the sodium lactate was present dominantly over the surface silicon and aluminium lactates. The incorporation of the $NaNO_3$ hugely decreased the content of isolated OH in the Na-SiO_2-Al_2O_3(35), as indicated by the comparative intensities of the isolated OH stretching bands between the Na-SiO_2-Al_2O_3(35) and $NaNO_3$/Na-SiO_2-Al_2O_3(35) (Fig. S10). The fact that the formation of the surface silicon and aluminium lactates is limited by the content of isolated OH is further supporting evidence that the isolated SiOH serves as a base to neutralize LA to form surface silicon lactate. With increasing temperature till 300 °C, the 1583 cm^{-1} band shifted to 1606 cm^{-1}, indicating that the sodium acrylate partially hydrolyzes. The 1606 cm^{-1} band is deemed to be overlapped of those of the sodium lactate as the major component and the surface silicon and aluminium lactates as the minor components. From 300 °C upwards, the 1606 cm^{-1} band remained unchanged in intensity even after 4 h of heating at 350 °C, which indicates that lactate hydrolysis can be suppressed under the weakly acidic condition. Meanwhile the principal band of the LA shifted to 1707 cm^{-1}, confirming the production of the AA. The strong chemical stability of the lactates is substantiated by the spectrum of a spent $NaNO_3$/Na-SiO_2-Al_2O_3(35) catalyst sample after 28 h of LA decarbonylation at 350 °C. A principal band of sodium lactate at 1593(s) cm^{-1} dominated while a principal one of surface silicon and aluminium lactates was deemed to be obscured by the broad 1593(s) cm^{-1} band, as in Fig. 7(g). The negligible presence of PLA and the strong chemical stability of the lactates are in accordance

with the low selectivity to PLA + coke and the strong catalytic stability for the production of AD, respectively over the weakly acidic $NaNO_3$/Na-SiO_2-Al_2O_3(35). By contrast, the *in situ* generated sodium lactate from LA displacement with the unsupported $NaNO_3$ (eqn (S1)) is thought to suffer from easy dehydration of the sodium lactate (eqn (S2)) which triggers the fast catalyst deactivation with polymerization of the sodium acrylate (eqn (S3), similar to the case with the unsupported KNO_3.[20,21] The chemical instability of the unsupported sodium lactate is evidenced by the spectrum of a spent unsupported $NaNO_3$ catalyst sample after 5 h of LA decarbonylation at 350 °C. The complex spectrum displayed three main bands at 1645(sh), 1587(s) and 1575(s) cm^{-1}, as in Fig. 7(h). The 1645(sh) and 1575(s) cm^{-1} bands are assigned to the signature features of poly(sodium acrylate),[79,80] and the 1587(s) cm^{-1} one corresponds to the principal feature of sodium lactate.[76,77] It is evident that substantial amounts of sodium lactate already transform to poly(sodium lactate) after 5 h of reaction, the catalyst severely deactivating. This accounts for the poor and unstable catalytic performance with the unsupported $NaNO_3$.

$$\mathbf{C_2H_4(OH)COOH + NaNO_3 \longrightarrow C_2H_4(OH)COONa + HNO_3} \quad \textbf{(S1)}$$

$$\mathbf{C_2H_4(OH)COONa \longrightarrow CH_2{=}CHCOONa + H_2O} \quad \textbf{(S2)}$$

$$\mathbf{nCH_2{=}CHCOONa \longrightarrow [CH_2{=}CHCOONa]_n} \quad \textbf{(S3)}$$

Pathways of the LA decarbonylation over catalyst systems

Scheme S1 illustrates the visualized catalytic cycle of the LA decarbonylation with SiO(H)Al as the assisting acid sites over sodium-containing SiO_2-Al_2O_3-based systems. The catalytic cycle starts with the Na^+ and SiO(H)Al as the catalytic active components. At first, LA displaces the Na^+ to generate the sodium lactate with the release of H^+. At second, the first SiO(H)Al site donates its H^+ to the sodium lactate. With the assistance of this H^+, the sodium lactate exchanges its Na^+ with the H^+ of the other SiO(H)Al site, which is the rate-determining step. Subsequently, the dehydration between the resultant LA and the first SiO(H)Al site takes place to give the corresponding ester $SiO(Al)COC_2H_4(OH)$. This unstable ester decomposes with the assistance of Na^+ and finally leads to the formation of AD and CO with the concomitant regeneration of the Na^+ and SiO(H)Al.

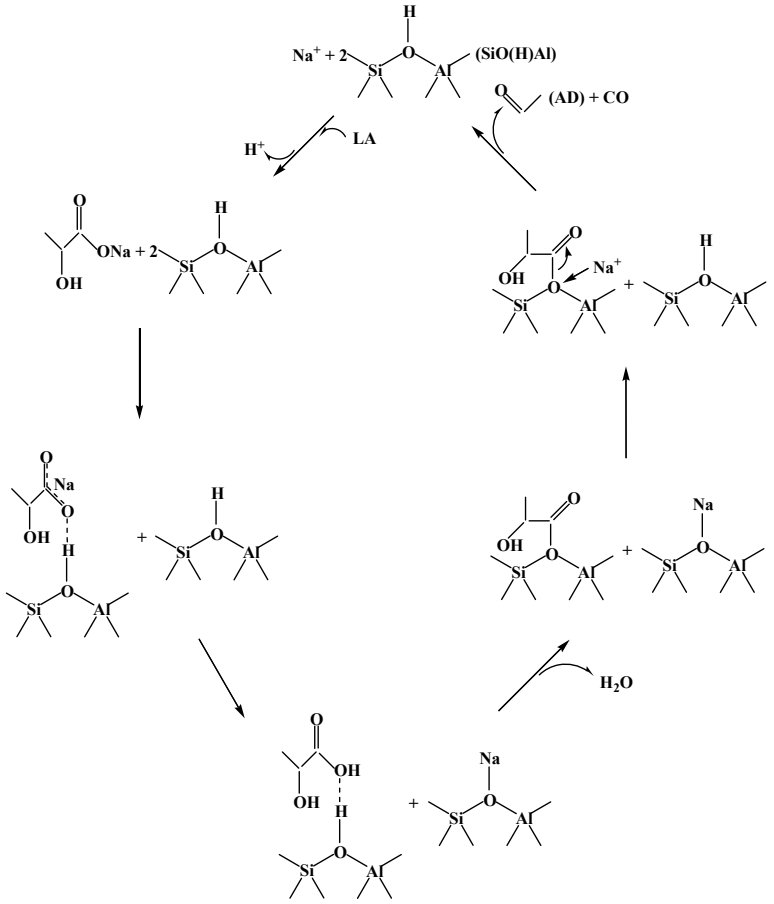

Scheme S1 Visualized catalytic cycle of the LA decarbonylation with SiO(H)Al as the assisting acid sites over sodium-containing SiO_2-Al_2O_3-based systems.

Experimental

Aqueous solution of 90 % LA was supplied by VWR Chemicals. AA (99 %), PA (99 %) and HA (95 %) were obtained from Alfa Aesar. 2,3-PD (97 %), AD (≥ 99.5%), HAc (≥ 99 %), EtOH (≥ 99.5 %), $NaNO_3$ (≥ 99 %), the Grade 15 SiO_2 and γ-Al_2O_3 were purchased from Sigma-Aldrich. The AEROSIL SiO_2 was supplied by Evonik.

The Grade 15 SiO_2, AEROSIL SiO_2 and γ-Al_2O_3 samples were subjected to 5 h of calcination in air at 540 °C followed by 24 h of rehydration in air at 22 °C before use. The Na-SiO_2-Al_2O_3 was prepared according to patent.[85] The as-prepared Na-SiO_2-Al_2O_3 was dried at 110 °C overnight. Except for the dried Na-SiO_2-Al_2O_3(35) sample, all the dried Na-SiO_2-Al_2O_3 samples were calcined in air at 540 °C for 5 h and rehydrated in air at 22 °C for 24 h before use.

The NH_4-SiO_2-Al_2O_3(35) was obtained by ion-exchanging a first portion of the dried Na-SiO_2-

Al_2O_3(35) sample twice with aqueous solutions of 0.5 M NH_4NO_3 at 80 °C for 17 h. The as-prepared NH_4-SiO_2-Al_2O_3(35) was filtered off, washed with deionized water and dried at 110 °C overnight before use. The H-SiO_2-Al_2O_3(35) was produced by calcination of a portion of the dried NH_4-SiO_2-Al_2O_3(35) sample in air at 540 °C for 5 h. The as-prepared H-SiO_2-Al_2O_3(35) was rehydrated in air at 22 °C for 24 h before use. The $NaNO_3$/Na-SiO_2-Al_2O_3(35) was prepared by incipient wetting impregnation. A second portion of the dried Na-SiO_2-Al_2O_3(35) sample was impregnated with an aqueous solution of $NaNO_3$. The initial molar ratio of the $NaNO_3$ to the Na in the dried Na-SiO_2-Al_2O_3(35) was set at 1.0, so that the initial Na/Al molar ratio in the $NaNO_3$/Na-SiO_2-Al_2O_3(35) actually attained to 6.2. The as-prepared $NaNO_3$/Na-SiO_2-Al_2O_3(35) was dried at 110 °C overnight and calcined in air at 540 °C for 5 h followed by 24 h of rehydration in air at 22 °C before use. Remaining portion of the dried Na-SiO_2-Al_2O_3(35) sample was calcined in air at 540 °C for 5 h and rehydrated in air at 22 °C for 24 h before use.

The catalytic vapour-phase LA decarbonylation reaction was conducted at 350 °C and 1 atm in the vertical, down-flow fixed-bed tubular reactor. The reactor body consisted of a stainless steel tube (59 cm long, 1.2 cm o.d. and 0.85 cm i.d.), which was mounted in a cylindrical electric furnace (45 cm long). The catalyst bed was sandwiched in the middle of the reactor with quartz wool. A bed of glass beads (*ca.* 1.0 g) was placed above the catalyst bed. Prior to the reaction, powder of each precatalyst sample was subjected to pelletizing at a pressure of 40 kN followed by sieving to 400-600 μm particles. A 0.50 g precatalyst sample (unless otherwise specified) was loaded in the reactor and subsequently pretreated with the carrier gas (N_2 + He) (N_2/He = 1/5 volumetric ratio) at a flow rate of 30 ml min^{-1} at 350 °C for 1 h. Afterwards, the 20 % LA aqueous solution was fed from the top of the reactor along with the carrier gas to start the reaction, the reactor temperature being kept at 350 °C. The liquid reaction mixture was condensed in an ice-water trap located at the outlet of the reactor. The collected liquid products were analyzed by offline HPLC on Shimadzu CTO-20A and offline GC on Agilent 6890N. Apart from known LA, AD, AA, PA, 2,3-PD, HAc, HA and EtOH, small amounts of unknown byproducts were detected in all the catalytic tests. These unidentified minor byproducts were not included in the carbon recovery. PLA and coke were analyzed by measuring weight gain of the spent catalyst sample. Conversion of LA and selectivity to liquid product were estimated following the formulae reported previously.[86] Selectivity to PLA + coke was estimated based on the average amount of carbon deposits measured by TGA in air of the spent catalyst sample after 5 h of reaction.

The IR spectroscopic experiments were performed on a BIO-RAD FTS 3000 MX FT-IR spectrometer. The KBr-diluted spent catalyst samples were made by mixing and grinding spent catalyst samples of *ca.* 1.1 mg each and KBr of *ca.* 80 mg each and then pressing them into wafers at a pressure of 40 kN. The spectra of the KBr-diluted sample wafers were measured under atmospheric Ar at 22 °C. The

precatalyst samples were ground and pressed into wafers of 20 mg each at a pressure of 40 kN. The LA reactivity and reaction intermediates on the precatalyst wafers were monitored in an atmosphere- and temperature-controllable IR cell at 22-350 ^{o}C. In a typical experiment, one of the precatalyst wafers was subjected to 0.5 h of thermal evacuation pretreatment under vacuum (10^{-2} mmHg) at 350 ^{o}C, except for the NH_4-SiO_2-Al_2O_3(35) which was treated under vacuum (10^{-2} mmHg) at 100 ^{o}C. The spectrum of the pretreated wafer was recorded under static vacuum at 22 ^{o}C as a background. Onto the pretreated wafer was added a small drop of the 20 % LA aqueous solution in air at 22 ^{o}C. The resultant sample wafer was evacuated under vacuum (10^{-2} mmHg) at 22 ^{o}C for up to 1.5 h. Afterwards, the sample wafer underwent thermal treatments at different temperatures under flowing N_2. After every thermal treatment, the sample wafer was evacuated (10^{-2} mmHg) at 22 ^{o}C for 0.5 h and the surface IR spectrum was recorded under static vacuum at 22 ^{o}C. The subtract surface spectrum was recorded by subtracting the contribution of the background. To make up a loss of water in the sample wafer due to evaporation during the monitoring experiment, a small drop of deionized water was added onto the sample wafer at the end of thermal treatment at each temperature from 100 ^{o}C upwards. The nature of surface acid sites on the precatalyst wafers was assessed by pyridine adsorption in an atmosphere- and temperature-controllable IR cell. In a typical experiment, one of the precatalyst wafers was first subjected to 0.5 h of thermal evacuation pretreatment under vacuum (10^{-2} mmHg) at 350 ^{o}C. The spectrum of the pretreated wafer was recorded under static vacuum at 22 ^{o}C as a background. Then the pretreated wafer was exposed to vapour of purified pyridine at 22 ^{o}C for 2 min for pyridine adsorption. Ideal pyridine chemisorption was obtained by pumping out (10^{-2} mmHg) at 200 ^{o}C for 0.5 h. The spectrum of chemisorbed pyridine was recorded under static vacuum at 22 ^{o}C against the background spectrum.

The acidity of the precatalysts was measured by NH_3-TPD on a Thermo Scientific TPROD 1100 instrument. In a typical measurement, a 0.10 g precatalyst sample in powder was pretreated in flowing He at 300 ^{o}C for 1 h, followed by adsorption of flowing 10 % NH_3 in He at 100 ^{o}C for 0.5 h. After the NH_3-adsorbing sample had been flushed with flowing He at 100 ^{o}C for 15 min, the TPD was performed from 100 to 850 ^{o}C in flowing He at a heating rate of 10 ^{o}C min^{-1}. During the whole experiment, the gas flow rate was set at 50 ml min^{-1}. The amount of desorbed NH_3 in stream was monitored by a thermal conductivity detector. Quantification of desorbed NH_3 was performed by calibration with the injection of 10 % NH_3 in He pulse at 22 ^{o}C. The acidity of the precatalyst was estimated from the integrated peak area relative to the average calibration value from a dozen of injections of the NH_3 pulse.

The thermogravimetric experiments were conducted on a TGA Q500 analyzer. The samples in powder were dried overnight at 110 ^{o}C prior to TGA. Under flowing purified air at 60 ml min^{-1}, the weight loss profiles of the dried samples of *ca.* 10 mg each were recorded from 30 to 800 ^{o}C at a heating

rate of 10 ^{o}C min^{-1}.

The elemental analysis was performed by inductively coupled plasma-optical emission spectroscopy (ICP-OES) on a Varian Vista-MPX CCD simultaneous ICP-OES spectrograph.

The BET surface areas and pore volumes of the precatalysts were measured by N_2 adsorption–desorption on a Quantachrome Autosorb-6B analyzer.

The physical properties of all the precatalysts used in this work are listed in Table S2.

Table S2 Physical properties of the precatalysts.

Precatalyst	BET surface area (m^2 g^{-1}) [a]	Pore volume (ml g^{-1}) [a]	Element content (%) [b]		
			Na	Si	Al
Grade 15 SiO_2	591	0.34	0.05		
AEROSIL SiO_2	295	1.5			
γ-Al_2O_3	147	0.21			
Na-SiO_2-Al_2O_3(5)	456	0.48	1.7	27	5.1
Na-SiO_2-Al_2O_3(23)	231	0.60	1.8	28	1.2
Na-SiO_2-Al_2O_3(35)	132	0.64	2.5	32	0.87
Na-SiO_2-Al_2O_3(75)	104	0.69	2.0	36	0.45
H-SiO_2-Al_2O_3(35)	136	0.62	0.010	34	0.93
$NaNO_3$/Na-SiO_2-Al_2O_3(35)	51.9	0.17	4.7	34	0.89

[a] Measured by N_2 adsorption-desorption. [b] Determined by ICP-OES.